An Unsaturated Soil Material Point Method for Simulating Rainfall-Induced Landslides

Long Zhu[1], Lele Wang[2], Xiao Liu[3], Wenyu Ye[2*]

[1]Department of Public Security Guizhou Police College (Guiyang), Guiyang, China
[2]School of Transportation Science and Engineering, Harbin Institute of Technology (Harbin), Harbin, China
[3]Yuxi Highway Engineering Quality Supervision Station (Yuxi), Yuxi, China

Abstract: Rainfall infiltration frequently triggers slope failures by elevating pore water pressure and compromising the shear strength of unsaturated soil layers. Modeling these severe geological events remains computationally challenging. Standard grid-based techniques, such as the Finite Element Method (FEM), typically fail due to severe mesh distortion under large deformations, whereas the Discrete Element Method (DEM) demands excessive computational resources. Addressing this gap, we develop an advanced theoretical framework utilizing the Material Point Method (MPM) integrated with a liquid-solid-gas three-phase mechanics model. We first verify the algorithmic accuracy using a 1D unsaturated soil column test. Subsequently, the framework is deployed to capture the dynamic displacement and mechanical responses of a 2D rainfall-induced landslide. Benchmarking against FEM data confirms that our multiphase MPM accurately models the infiltration process and subsequent structural collapse. Ultimately, this approach offers a highly robust computational strategy for analyzing large-scale landslide deformations and improving predictive assessments.

1. Introduction

Across China, geological hazards are both widespread and highly frequent, leading to recurrent outbreaks that inflict severe social and economic damage. Statistical data indicates that slope failures constitute more than 70% of these geological events, with rainfall acting as the triggering mechanism in roughly 90% of cases [1]. Due to highly complex natural geological conditions alongside rugged, mountainous, and hilly terrains, the southwestern region and the Three Gorges Reservoir area remain exceptionally vulnerable to rainfall-induced landslides [2]. Prominent instances of this include the Lanbazi landslide located in Xintian Town, Wanzhou District, as well as the Qianjiangping landslide within the Three Gorges Reservoir zone, both of which resulted in immense economic losses and severe casualties [3]. From a mechanical perspective, the internal mechanism of these rainfall-triggered events is driven by rainwater infiltrating the shallow soil layers, which transforms the initially dry granular material into an unsaturated medium. This infiltration process subsequently elevates the internal pore water pressure and diminishes the effective stress, ultimately causing a drastic reduction—or even a total loss—of the soil's shear strength.

Over the past several decades, domestic and international scholars have proposed a variety of analytical techniques to accurately evaluate stability and deeply investigate the deformation and failure mechanisms of landslides. Early investigations into slope stability relied heavily on semi-theoretical and semi-empirical limit equilibrium frameworks, including the Janbu method, the Spencer method, and the modified Bishop approach. However, because limit equilibrium theories generally treat the sliding mass purely as a rigid body and lack a comprehensive integration of stress-strain characteristics, they struggle to accurately reflect the complete physical evolution of a landslide [4]. Driven by the rapid advancement of computational technology, numerical simulation has gradually emerged as the mainstream strategy for evaluating landslide stability. While the Finite Element Method (FEM) can effectively manage complex geometric boundaries and partially account for the heterogeneity of geotechnical masses, it is highly susceptible to computational non-convergence and severe mesh distortion when attempting to solve large deformation problems [5]. Alternatively, the Discrete Element Method (DEM) [6,7] better compensates for the inherent limitations of continuous media during massive deformations; yet, it continues to face numerous unresolved difficulties regarding the determination of energy dissipation and damping parameters. Other approaches, such as Fast Lagrangian Analysis of Continua (FLAC) [8,9], Discontinuous Deformation Analysis (DDA) [10], and various mesh-free methods [11], have certainly demonstrated specific advantages within their respective domains. Nonetheless, they all exhibit varying degrees of limitation concerning overall numerical stability, computational efficiency, and boundary condition processing.

zlong@alu.hit.edu.cn, 24s132083@stu.hit.edu.cn, ssyycc2026@163.com, *24b932012@stu.hit.edu.cn

© The Authors, published by EDP Sciences. This is an open access article distributed under the terms of the Creative Commons Attribution License 4.0 (https://creativecommons.org/licenses/by/4.0/).

To overcome these specific grid-based limitations, researchers have increasingly turned to the Material Point Method (MPM) [12,13]. Utilizing a hybrid Lagrangian-Eulerian description, this particle-based approach has recently shown exceptional promise in modeling severe landslide deformations. MPM not only retains the advantages of continuous medium methods in boundary processing but also fundamentally avoids the mesh distortion issues inherent in FEM, showing significant superiority in simulating large landslide deformations and fluid-structure coupling processes. While the Material Point Method (MPM) successfully circumvents the severe mesh distortion inherent in the Finite Element Method (FEM) during large deformations, it generally incurs a higher computational cost. Qualitatively, for the 2D landslide scenario presented in this study, the US-MPM required more computational time than the traditional FEM. This increased demand primarily stems from the continuous, bidirectional data mapping between the moving Lagrangian material points and the fixed Eulerian background grid at each computational step. However, this computational trade-off is highly justifiable; whereas FEM simulations typically terminate prematurely during the large deformation phase due to grid entanglement, the US-MPM robustly captures the complete post-failure kinematics without requiring complex remeshing algorithms. However, existing MPM research predominantly focuses on dry or fully saturated soils. Numerical simulation studies addressing unsaturated soil landslides triggered by rainfall remain scarce, and the relevant theoretical models urgently need improvement. On another note, landslide prediction, as a core component of disaster risk reduction, has evolved from empirical predictions [14], statistical predictions, and nonlinear dynamic predictions to comprehensive multi-model fusion predictions. In statistical prediction, for example, Zhao [15] proposed an empirical formula for estimating the maximum horizontal distance of high-speed long-runout landslides. Yet most existing prediction models lack clear physical and mechanical meanings, failing to truly reveal the intrinsic mechanisms of landslide evolution, and exhibit obvious deficiencies in the dynamic updating and utilization efficiency of real-time monitoring data [16].

Addressing the aforementioned theoretical and practical shortcomings, this paper proposes a theoretical and algorithmic framework for an Unsaturated Soil Material Point Method (US-MPM) suitable for rainfall-induced landslides. This framework is based on the fundamental MPM algorithm coupled with a liquid-solid-gas three-phase unsaturated porous medium theory. This study first verifies the correctness and effectiveness of the algorithm through a one-dimensional unsaturated soil column numerical example, and subsequently applies it to simulate the entire deformation and failure process of a two-dimensional rainfall-induced landslide, conducting an in-depth comparison with FEM calculation results. This research aims to provide a reliable numerical simulation tool for analyzing rainfall infiltration in unsaturated landslides and to lay a solid mechanical theory foundation for constructing intelligent landslide prediction models based on dynamic monitoring data.

2. Methods

2.1. Multiphase Representation in MPM

Soil is a complex mixture comprising solid, liquid, and gas phases, and the interactions among them determine the hydraulic response of the soil [17]. In the proposed three-phase single-point method, the unsaturated porous medium is assumed to be a mixture composed of a solid skeleton and pore fluids, namely liquid and gas [18]. When a single material point is used to represent the three phases simultaneously, its total volume is composed of the respective volumes of the three phases, as illustrated in Fig. 1, expressed mathematically as Eq.(1).

$$V_{MP} = \sum_{ph} V_{ph} = V_s + V_l + V_g \tag{1}$$

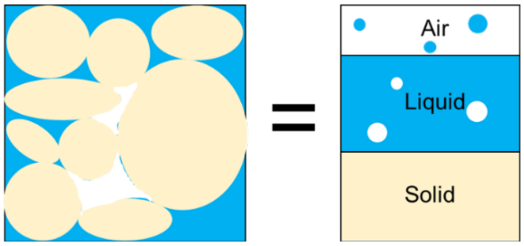

Fig 1. Scheme of three-phase medium

The volume fraction of each phase, denoted as n_{ph}, can be further derived based on the relationship between porosity and saturation, where $n_s = 1-n$, $n_l = nS_l$, and $n_g = nS_g$, with n representing the porosity, and S_l and S_g representing the fluid and gas saturations, respectively.

2.2. Governing Equations

To accurately simulate the dynamic responses within unsaturated porous media, our framework relies on the core laws of physics: the conservation of momentum and mass. We derive the momentum balance relationships for the gas, liquid, and overall mixture by explicitly keeping the relative accelerations and velocities of the pore fluids in the calculations. Following this logic, the specific equation governing gas momentum conservation is detailed in Eq. (2).

$$\rho_g \dot{u}_g = \nabla p_g - \frac{nS_g \mu_g}{\kappa_g}(\dot{u}_g - \dot{u}_s) + \rho_g b \tag{2}$$

Similarly, the liquid momentum conservation equation is given by Eq. (3).

$$\rho_l \dot{u}_l = \nabla p_l - \frac{nS_l \mu_l}{\kappa_l}(\dot{u}_l - \dot{u}_s) + \rho_l b \tag{3}$$

The mixture momentum conservation equation combines these components and is expressed as Eq. (4).

$$n_s \rho_s \dot{u}_s + n_l \rho_l \dot{u}_l + n_g \rho_g \dot{u}_g = \nabla \cdot \sigma + \rho_m b \tag{4}$$

For mass conservation, the formulation rigorously accounts for mass exchange between fluids, such as the evaporation and condensation of water in the pores, ensuring an accurate mathematical description of the multiphase flow dynamics.

2.3. Constitutive and Hydraulic Models

For elastoplastic soil materials, the stress of the unsaturated soil can be represented using net stress and matric suction as state variables. The material constitutive model adopts the modified Mohr-Coulomb yield criterion to accurately describe the influence of fluid pressure on the yield surface, represented as $q = c\cos\varphi + \bar{p}\sin\varphi$. It is important to note that the cohesion and internal friction angle in unsaturated soils are directly affected by matric suction, which is defined as the difference between gas and liquid pressures ($s = p_g - p_l$). Furthermore, for the saturation of the unsaturated porous medium, the traditional water retention curve, specifically the van Genuchten model, is employed to establish its relationship with gas and liquid pressures.

2.4. Explicit Integration Scheme

Our numerical approach relies on a forward time difference format within an explicit Update Stress First (USF) integration scheme to evaluate multiphase stress and strain. We represent the solid continuum using a collection of Lagrangian material points. Each point tracks its own mass, spatial position, volume, velocity, and stress while moving independently across a fixed Eulerian computational mesh. The overall computational procedure is schematically depicted in Fig. 2. At the start of a calculation step, shape functions interpolate this particle data onto the nodal points of the background grid. The system then resolves the governing equations at the grid level. Finally, the updated kinematic and stress values are pushed back to the material points. Discarding the temporarily deformed grid at the conclusion of each timestep guarantees that mesh entanglement and distortion never occur.

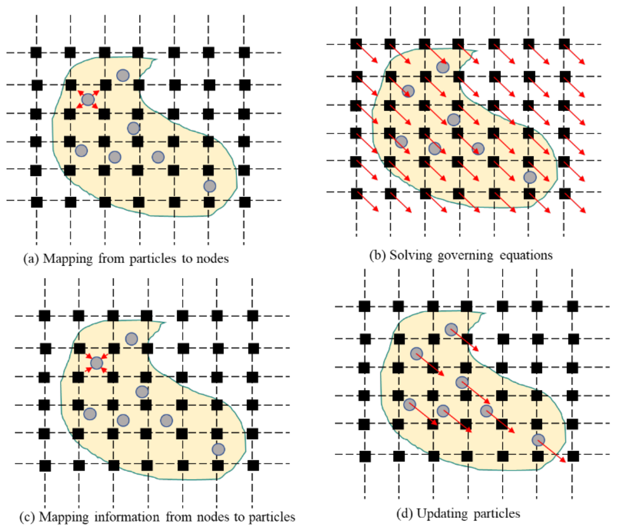

Fig. 2. Schematic diagram of material point method

3. Analysis and Discussion of Test Results

3.1. One-Dimensional Unsaturated Soil Column Validation

The present study validates the proposed algorithm's accuracy and performance using a 1D unsaturated soil column test. The geometric model stands 1000 mm tall and 50 mm wide. To properly simulate the physical constraints, we restrict flow at the bottom and along both sides, rendering them completely impermeable. Rainwater enters exclusively through the top surface, where the constant infiltration rate is fixed at 1.0×10^{-4} m/s. The computational model and particle discretization are illustrated in Fig. 3.

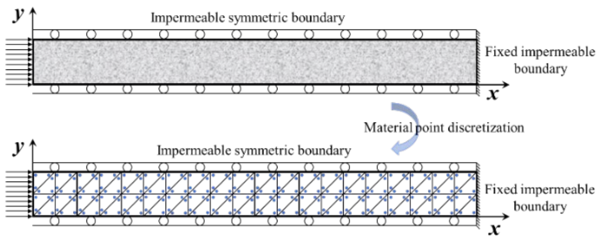

Fig. 3. Computational model and particle discretization

Comparing vertical profiles across multiple time intervals (20s, 80s, 160s, 320s, and 600s) reveals a strict agreement between our US-MPM calculations and standard FEM outputs. In the initial infiltration phase, surface matric suction deteriorates. The soil surface rapidly saturates as pore water pressure climbs toward zero. Trapped by the impermeable boundaries, the accumulating water has nowhere to drain, triggering a steady rise in excess internal pore pressure. At exactly 600s, complete column saturation occurs, forcing the pore water pressure into a strictly linear vertical distribution. The pore water pressure and saturation profiles at different times are presented in Fig. 4. Such precise alignment with established FEM data ultimately confirms that the US-MPM is both physically realistic and algorithmically robust.

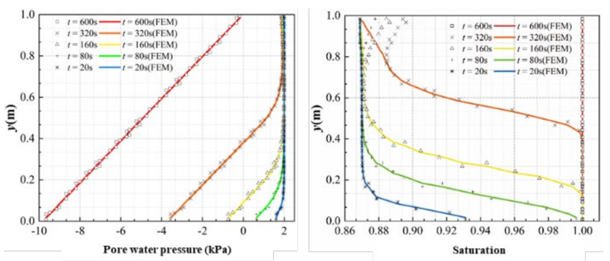

Fig. 4. Comparison of pore water pressure and saturation

3.2. Two-Dimensional Rainfall-Induced Landslide Simulation

To test the method against complex failure mechanics, the landslide infiltration process reduces to a 2D plane strain problem. Rainwater enters the slope at a constant 0.012 m/h over a 36-hour window. The computational model of the slope is illustrated in Fig. 5. For the numerical setup, 3858 triangular elements define the MPM domain, with three material points assigned to each element. On the other hand, the baseline FEM model relies on 1222 quadrilateral elements.

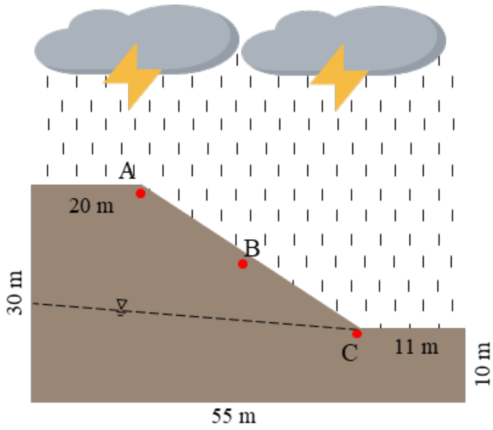

Fig. 5. Slope Computational model

To ensure full model reproducibility, the mechanical and hydraulic boundary conditions of the 2D slope are explicitly defined. Mechanically, the base of the model is fully fixed, restricting displacements in both the horizontal and vertical directions, while the lateral boundaries are roller-supported to constrain horizontal movement. Hydraulically, the base and the upper portions of both lateral sides are assumed to be strictly impermeable, whereas the lower portions of the lateral boundaries are set as linear water pressure boundaries. The slope surface is initially configured as a negative pressure boundary to simulate the existing matric suction; during the simulation, this is subsequently converted into an infiltration boundary subjected to a constant rainfall rate of 0.012 m/h over the 36-hour period. The material parameters adopted in this simulation are summarized in Table 1.

Table 1. Material parameters of slope

Property Name	Parameter Value
material type	Unsaturated porous medium
Soil density [kg/m³]	1800
Liquid density [kg/m³]	1000
Permeability coefficient [m/h]	0.36
Constitutive model	Mohr-Coulomb model
Poisson's ratio	0.3
Elastic modulus [kPa]	10,000
Cohesion [kPa]	12
Internal friction angle [deg]	30
Liquid water retention curve	van Genuchten model
Residual saturation	0
α [1/kPa]	0.04
Nw	1.2
l	0.5
Permeability coefficient curve	constant model

After 36 hours of continuous rainfall, seepage nearly saturates the surface pores. In contrast, the deeper soil remains relatively dry, matching field observations of actual landslide infiltration. Pore water pressure behaves inversely to this saturation profile. Because the shallow soil saturates so quickly, surface pore pressure drops toward zero, leaving it noticeably lower than the interior. Both the MPM and FEM simulations place the dividing line between this shallow low-pressure zone and the deeper high-pressure core roughly 4 meters below the slope surface. Mechanically, this surface saturation destroys local shear strength. The internal soil, however, grips tighter thanks to residual matric suction. As a direct result, the outer layer begins to slide. We recorded peak displacements of 0.016 m at the slope crest and 0.018 m down at the toe. The contour maps of pore water pressure, saturation, and displacement at t = 600 s are presented in Fig. 6.

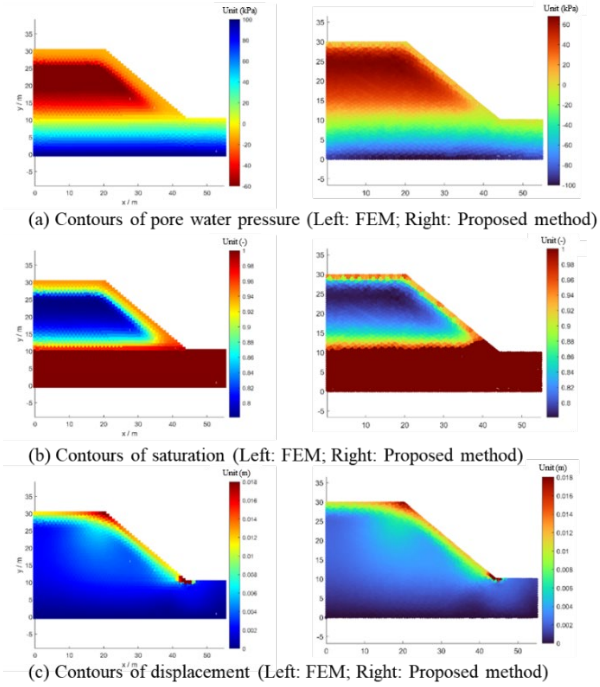

Fig. 6. Pore Pressure, Saturation, and Displacement Contour Map at t=600s

The simulation tracked specific metrics at three internal monitoring locations (points A, B, and C), as illustrated in Fig. 7. The MPM and FEM outputs aligned almost perfectly. For pore water pressure, the peak absolute error reached just 3.517 kPa, yielding a relative error of only 0.108. Saturation levels showed a maximum absolute deviation of 0.021. Even more strictly, physical displacement differed by no more than 1.134 mm across the two models. These incredibly tight margins confirm that both methods match. Beyond the error metrics, the simulation captured the exact collapse mechanism. As the rain continues, internal pore dynamics shift entirely. The soil transitions from absorbing water (suction) to expelling it (repulsion), with pore pressure hitting a floor of roughly -12 kPa. This specific threshold proves critical. It strips away effective stress and severely degrades the soil's shear strength, leaving gravity to pull the weakened mass downward.

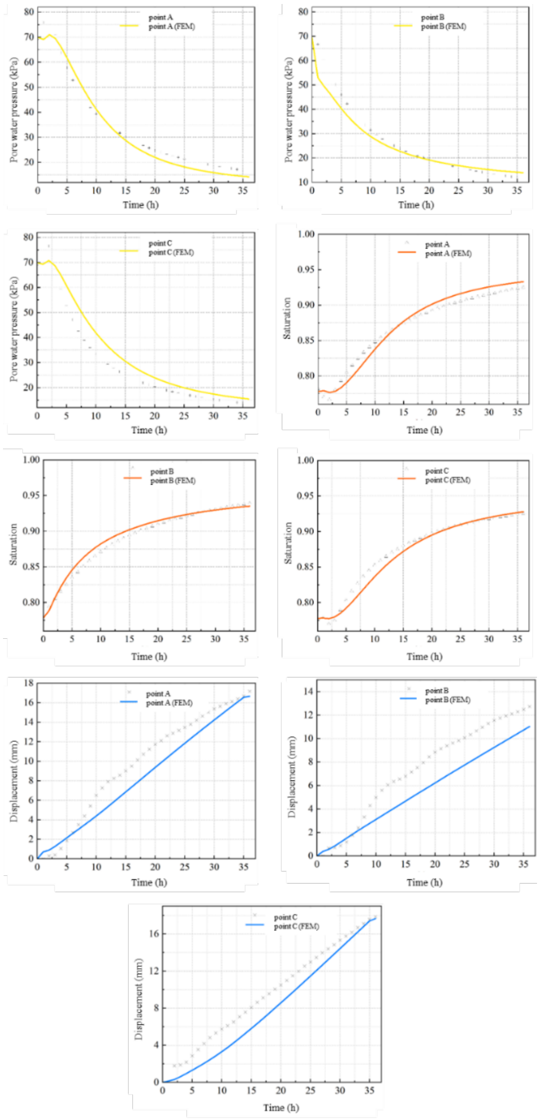

Fig. 7. Comparison Chart of Monitoring Point Curves

4. Conclusion

This research formulated an explicit Unsaturated Soil Material Point Method (US-MPM) to decode how rainfall triggers complex multiphase landslides.

(1) The mathematical core relies on liquid-solid-gas three-phase mechanics. By rigorously discretizing the multiphase momentum equations across moving particles, we built a dedicated Update Stress First (USF) integration scheme. This specific setup effectively tracks fluid pressure shifts and dynamic soil-water interactions.

(2) A 1D unsaturated soil column test proved the algorithm's baseline accuracy. Tracking both pore water pressure and saturation revealed tight alignment with standard FEM models, verifying that the new framework handles complex seepage without issue.

(3) Scaling the model to a full 2D landslide exposed the exact physical breakdown. Continuous water infiltration clearly eroded matric suction, drove up surface pore pressures, and subsequently destroyed the soil's shear strength. Because it entirely avoids the mesh entanglement seen in traditional grid methods, this US-MPM approach offers a highly stable numerical foundation for building smarter landslide early warning systems.

Acknowledgment

This research was supported by the 2024 Natural Science Research Project of the Department of Education of Guizhou Province (Young Scientific and Technological Talent Growth Project), Grant No. [2024] 184.

References

1 F. Guzzetti, S. L. Gariano, S. Peruccacci, M. T. Brunetti, and M. Melillo, "Rainfall and landslide initiation," in Elsevier eBooks, 2022, pp. 427–450. doi: 10.1016/b978-0-12-822544-8.00012-3.

2 K. Wang and S. Zhang, "Rainfall-induced landslides assessment in the Fengjie County, Three-Gorge reservoir area, China," Natural Hazards, vol. 108, no. 1, pp. 451–478, Mar. 2021, doi: 10.1007/s11069-021-04691-z.

3 B. Qin, J. Zou, X. Wang, L. Yang, and P. Lv, "Landslide susceptibility evaluation using multiple machine learning models: a case study of Wanzhou District in the Three Gorges Reservoir area," Geological Journal, Oct. 2025, doi: 10.1002/gj.70104.

4 L. Yang, Y. Wang, T. Glade, and J. Liu, "From theory to practice: force-energy equilibrium analysis for assessing failure extension lengths in excavation-induced translational landslides," Bulletin of Engineering Geology and the Environment, vol. 84, no. 2, Jan. 2025, doi: 10.1007/s10064-025-04092-7.

5 A. Aalianvari and S. Jahanmiri, "Fluid flow modeling in fractured rocks using human mental search optimization," Geotechnical and Geological Engineering, vol. 43, no. 6, Jul. 2025, doi: 10.1007/s10706-025-03223-x.

6 F. Guo, E. Zhen, A. Wang, and L. Wang, "Research on discrete element method for geometric nonlinear problems in continuum medium plate and shell structures," Mechanics of Solids, vol. 60, no. 5, pp. 4123–4148, Oct. 2025, doi: 10.1134/s0025654425602848.

7 H. Ma et al., "A review of the Discrete Element Method (DEM) simulation of mineral Comminution Processes: Part I. Theoretical Developments," MetaResource, vol. 2, no. 4, pp. 257–283, Dec. 2025, doi: 10.23919/metar.2025.000016.

8 A. Kumar and L. B. Roy, "Analysis of slope failure in Ostapal open pit chromite mine using numerical modelling in FLAC—A case study," Indian Geotechnical Journal, Feb. 2025, doi: 10.1007/s40098-025-01200-y.

9 S. Li, B. Dai, Y. Hou, and D. Li, "Spatiotemporal stability responses of tunnel excavation under cyclical footage impact: a FLAC3D-Based Numerical study," Applied Sciences, vol. 15, no. 14, p. 7661, Jul. 2025, doi: 10.3390/app15147661.

10 Z. Chen, Z. Chen, T. Guo, W. Chen, Q. Zhang, and Z. Wu, "Depth-guided DIC for 3D shape, deformation, and strain measurement on discontinuous surfaces," Optics Express, vol. 33, no. 5, p. 11638, Feb. 2025, doi: 10.1364/oe.557594.

11 M. Aleyaasin, "Comparing the accuracy and sensitivity of Mesh-Free and finite element methods in vibration analysis," Dynamics, vol. 5, no. 2, p. 13, Apr. 2025, doi: 10.3390/dynamics5020013.

12 C. Zhou, Q. Zhong, X. Zhou, X. Wu, and S. Chen, "Research advances in large deformation analysis and

applications of the material point method," Applied Sciences, vol. 15, no. 12, p. 6617, Jun. 2025, doi: 10.3390/app15126617.

13 H. Ma, J. Li, Z. Sun, and X. Zhang, "An efficient arbitrary grid material point method for problems with nonconforming boundary conditions," International Journal for Numerical Methods in Engineering, vol. 126, no. 11, Jun. 2025, doi: 10.1002/nme.70054.

14 Y. Cao et al., "Unstructured moving least squares material point methods: a stable kernel approach with continuous gradient reconstruction on general unstructured tessellations," Computational Mechanics, vol. 75, no. 2, pp. 655–678, Jul. 2024, doi: 10.1007/s00466-024-02524-x.

15 W. Zhao, X. Xia, X. Su, Q. Liang, X. Liu, and N. Ju, "Movement process analysis of the high-speed long-runout Shuicheng landslide over 3-D complex terrain using a depth-averaged numerical model," Landslides, vol. 18, no. 9, pp. 3213–3226, Jun. 2021, doi: 10.1007/s10346-021-01695-5.

16 K. Bhuyan et al., "Generating multi-temporal landslide inventories through a general deep transfer learning strategy using HR EO data," Scientific Reports, vol. 13, no. 1, p. 162, Jan. 2023, doi: 10.1038/s41598-022-27352-y.

17 E. Wang, R. M. Cruse, Y. Zhao, and X. Chen, "Quantifying soil physical condition based on soil solid, liquid and gaseous phases," Soil and Tillage Research, vol. 146, pp. 4–9, Mar. 2015, doi: 10.1016/j.still.2014.09.018.

18 D. M. Pedroso, Y. Zhang, and W. Ehlers, "Solution of Liquid–Gas–Solid coupled equations for porous media considering dynamics and hysteretic retention behavior," Journal of Engineering Mechanics, vol. 143, no. 6, Feb. 2017, doi: 10.1061/(asce)em.1943-7889.0001208.